

1

Self-organized and self-assembled structures

Almost all systems we encounter in nature possess some sort of form or structure. It is then natural to ask how such structure arises, and how it changes with time. Structures that arise as a result of the interaction of a system with a template that determines the pattern are easy to understand. Lithographic techniques rely on the existence of a template that is used to produce a material with a given spatial pattern. Such pattern-forming methods are used widely, and soft lithographic techniques are being applied on nanoscales to produce new materials with distinctive properties (Xia and Whitesides, 1998). Less easily understood, and more ubiquitous, are self-organized structures that arise from an initially unstructured state without the action of an agent that predetermines the pattern. Such self-organized structures emerge from cooperative interactions among the molecular constituents of the system and often exhibit properties that are distinct from those of their constituent elements. These pattern formation processes are the subject of this book.

Self-organized structures appear in a variety of different contexts, many of which are familiar from daily experience. Consider a binary solution composed of two partially miscible components. For some values of the temperature, the equilibrium solution will exist as a single homogeneous phase. If the temperature is suddenly changed so that the system now lies in the two-phase region of the equilibrium phase diagram, the system will spontaneously form spatial domains composed of the two immiscible solutions with a characteristic morphology that depends on the conditions under which the temperature quench was carried out. The spatial domains will evolve in time until a final two-phase equilibrium state is reached. The evolution of such structures is governed by thermodynamic free energy functions, suitably generalized to account for the heterogeneity of the medium and the existence of interfaces separating the coexisting phases. The spontaneous formation of such structures is the system's response to an initial instability or metastability (Bray, 1994; Debenedetti, 1996; Dattagupta and Puri, 2004).

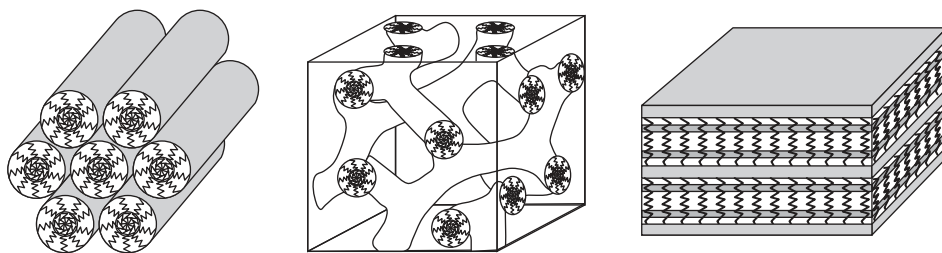


Fig. 1.1. Schematic depictions of hexagonal, gyroid and lamellar nanocomposites that result from the self-assembly of diacetylenic surfactants on silica. From Brinker (2004), p. 631, Figure 6a.

The formation of macroscopic coherent spatiotemporal structures arising from an initial instability or metastability is often a consequence of some inherent symmetry-breaking element. Fluctuations and conservation laws also play an important role in determining the character of the time evolution leading to self-organized structures. As the system evolves, interfaces which delineate the boundaries of local domains also move: thus an understanding of interface dynamics, and more generally of defect dynamics, is a central feature of the evolution of self-organized structures.

Ultimately, self-organized structures have their origin in the nature of the intermolecular forces that govern the dynamics of a system. In some instances, the connection between the macroscopic coherent structure and specific features of the intermolecular forces is rather direct. Self-assembly of molecular constituents in solution is such a process. Self-assembly leads to a variety of three-dimensional structures: strong hydrophobic attraction between hydrocarbon molecules can cause short chain amphiphilic molecules to organize into spherical micelles, cylindrical rod-like micelles, bilayer sheets, and other bicontinuous or tri-continuous structures (Fig. 1.1) (Gelbart *et al.*, 1994; Grosberg and Khokhlov, 1997; Brinker, 2004; Ozin and Arsenault, 2005; Pelesko, 2007). Self-assembly of long-chain block copolymers can also occur through microphase separation as a result of covalent bonds between otherwise immiscible parts of the polymer. This process can lead to three-dimensional structures with topologies similar to those of amphiphilic molecules (Fredrickson and Bates, 1996; Bates, 2005). Similarly, two-dimensional systems, such as Langmuir monolayers at a water–air interface or uniaxial ferromagnetic films, can self-assemble into unidirectional periodic stripes and hexagonally arranged circular drops as a result of the competition between long-range repulsive dipolar interactions and relatively shorter-range attractive van der Waals interactions. Monolayers on a metallic substrate can also self-organize into ordered structures (Fig. 1.2). The most direct way to model such self-assembly is by following the motions of the constituent elements by molecular dynamics. A number of different coarse-grain schemes have been devised in order to extend the size,

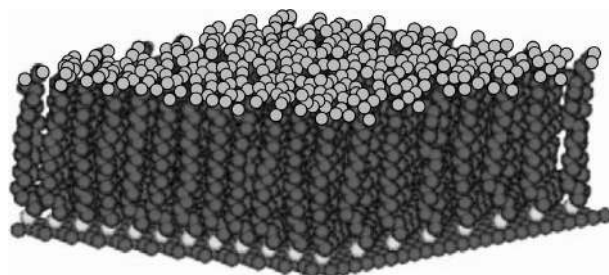


Fig. 1.2. Results of a molecular dynamics simulation of a densely packed assembly of 16-mercapto-hexadecanoic acid molecules tethered to a gold surface. From Lahann and Langer (2005), p. 185, Figure 2.

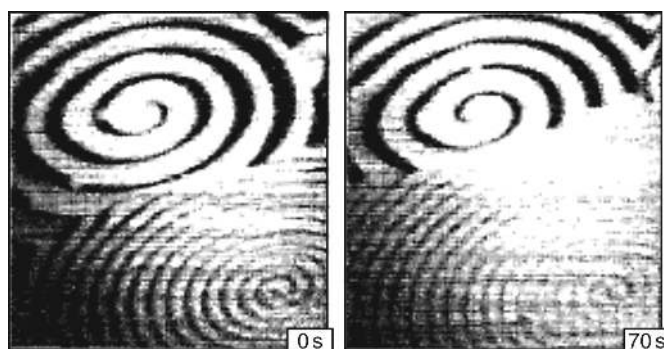


Fig. 1.3. Spiral wave CO oxidation patterns on the surface of a Pt(110) surface. Reprinted with permission from Nettesheim *et al.* (1993). Copyright 1993, American Institute of Physics.

length, and timescales of such simulations (Karttunen *et al.*, 2004; Nielsen *et al.*, 2004; Venturoli *et al.*, 2006). On mesoscopic scales self-assembly can be analyzed and understood through models based on free energy functionals and relaxational dynamics.

Self-organized structures also arise in systems that are forced by external flows of matter or energy to remain far from equilibrium (Nicolis and Prigogine, 1977; Kapral and Showalter, 1995; Walgraef, 1997; Manrubia *et al.*, 2004; Hoyle, 2006; Pismen, 2006). If chemical reagents are continuously supplied to and removed from a container where an oxidation reaction takes place on a catalytic surface, in many circumstances the chemical reaction does not occur homogeneously over the entire surface but instead proceeds by the propagation of chemical waves of oxidation that travel across the catalytic surface. The combination of nonlinear chemical kinetics and conditions that force the reaction to occur in far-from-equilibrium conditions is responsible for the existence of the evolving patterns of chemical waves seen on the surface of the catalyst (Fig. 1.3).

Biological systems almost always operate under far-from-equilibrium conditions since input of chemical and other energy sources is needed to maintain the living state. Consequently, the conditions for the appearance of self-organized structures are present in these systems. Indeed, the nonlinear chemistry associated with biochemical networks, in combination with diffusion of chemical species, can lead to the formation of chemical waves which are often implicated in the mechanisms responsible for biological function (Winfree, 1987, 2001; Murray, 1989; Goldbeter, 1996). Chemical waves are known to play a role in cell signaling processes leading to cell division, aggregation processes in colonies of the amoeba *Dictyostelium discoideum*, and the pumping action of the heart, to name a few examples. Perhaps even more interesting is the fact that chemical patterns have been observed in individual living cells (Petty *et al.*, 2000).

Although applications to fluid dynamics are not considered in this book, fluid flow also provides many examples of self-organized structures (Cross and Hohenberg, 1993; Frisch, 1995; Nicolis, 1995; Walgraef, 1997). The hexagonal patterns arising from Rayleigh–Bénard convection when a fluid is heated from below are familiar, as are the complex spatiotemporal patterns seen in turbulent fluids. In such cases, descriptions of the origins and dynamics of the patterns are usually based on an analysis of the Navier–Stokes equation; the instabilities are seen to emerge as a result of the convective nonlinear terms in this equation.

In contrast to equilibrium systems, in far-from-equilibrium systems free energy functions do not always exist, and the description of the dynamics of self-organized structures must be based on different premises. In the case of chemical and biochemical systems the starting point is usually a reaction–diffusion equation, while, as noted above, for fluid dynamics problems the Navier–Stokes equation is a natural starting point for the analysis.

In spite of the fundamental differences in the origins of diverse self-organized structures, there are often superficial similarities in their forms, and there exist common basic elements which are needed to understand their formation and evolution. At the macroscopic level, one needs a description in terms of suitable field variables or order parameters that account for the existence of spatial structure in the system. Other common elements include the presence of interfaces that separate phases or spatial domains that constitute the self-organized structure, and the existence of defects in the medium. Both of these features often control the dynamical evolution of the structure on certain time scales.

During the second half of the twentieth century, the concept of universality played a major role in our understanding of structural correlations and dynamics in condensed matter systems. Starting with Landau’s unifying concept of the order parameter (Landau, 1937) and culminating in the renormalization group theory of critical phenomena (Wilson and Kogut, 1974), these developments demonstrated

that a description of the relevant physics does not necessarily lie at the smallest available length or time scales for many fundamental problems. In many instances, the description of the dynamics of self-organized structures in nonequilibrium systems can be examined within a similar context. Consequently, often a macroscopic perspective may be adopted to describe the dynamics of these structures. Even for situations such as self-assembly where the crucial role of the underlying intermolecular forces is evident, the nature and dynamics of the self-assembled structures on long distance and time scales can be captured by approaches based on suitably defined field variables. While the use of such a perspective limits the spatial and temporal scales on which the description is valid, it is general enough to provide a basis for understanding most of the commonly observed structures, even on mesoscopic scales.

In the chapters that follow we describe the dynamics of self-organized structures based on equations of motion for order parameter fields, which provide a description of systems at the mesoscopic and macroscopic levels. Equations of motion for such order parameter fields can be constructed for systems described by free energy functionals, as well as for systems which are constrained to lie far from equilibrium, for which no such functionals exist. Such formulations enable one to identify similarities in both the forms of the self-organized structures and features that determine their evolution in equilibrium and far-from-equilibrium systems.

We begin with an analysis of the familiar phenomenon of phase segregation following a quench of a system into the two-phase region of the phase diagram. An essential ingredient in the dynamics is the behavior of interfaces separating domains of coexisting phases, and we develop a description of such interface dynamics. Domain segregation is modified when long-range repulsive interactions exist: the theoretical description of these systems is considered. In the far-from-equilibrium regime, the order parameter equations are constructed on the basis of weakly nonlinear theory where crucial slow modes are identified in the dynamics. Once again interfaces and fronts play an important role in determining the evolution of the system. Because of the lack of a free energy functional, a much richer variety of self-organized structures is observed, which includes structures with periodic or chaotic temporal behavior. While no truly unified picture of diverse self-organizing structures is possible, the presentation in this book provides the tools needed to analyze and understand the origins of various types of self-organized structure. The material should permit one to see similarities in the structures observed in nonequilibrium and driven systems, and draw parallels in the methods used to describe the phenomena.

2

Order parameter, free energy, and phase transitions

The kinetics of first-order phase transitions involves the separation of an initially one-phase system into two coexisting phases. The formation and coarsening of domains of the coexisting phases as the system evolves are of central interest. The phase segregation process is usually studied by first preparing the system in a region of the phase diagram where the homogeneous state is stable. The system is then suddenly quenched into the two-phase region, and segregation into domains of the two stable phases takes place. Such phase segregation arises in a variety of physical contexts, including binary alloys and fluid mixtures, ferromagnetic systems, superfluids, polymer mixtures, and chemically reacting fluids. The temperature–composition (T, c) phase diagram for a binary mixture composed of constituents A and B is shown in Fig. 2.1. For low enough temperatures, in the region bounded by the coexistence curve the binary mixture will segregate into A -rich and B -rich phases.

A quench that takes the system from a homogeneous to a two-phase region is often performed by changing temperature suddenly at fixed concentration. Such a quench from the one-phase state at high temperatures may be carried out either along the critical isoconcentration line that passes through the critical point (path a), or along off-critical paths (path b). Phase segregation may be monitored by the changes in the local concentration of the binary mixture. In general, the variable that signals the passage from the one-phase to two-phase regions is called the order parameter ϕ .

The kinetics of the phase separation process in a binary mixture is often discussed in terms of a free energy function $f(c)$. In the one-phase region the free energy function has a simple single minimum, while it is bistable in the two-phase region (Fig. 2.2). The chemical potential is defined as $\mu = (\partial f / \partial c)_{T, \rho}$. In mean field descriptions based on the free energy function, the spinodal line (dashed line in Fig. 2.1) is defined as the locus of points where the derivative of the chemical potential with respect to the concentration is zero. The definition of the spinodal

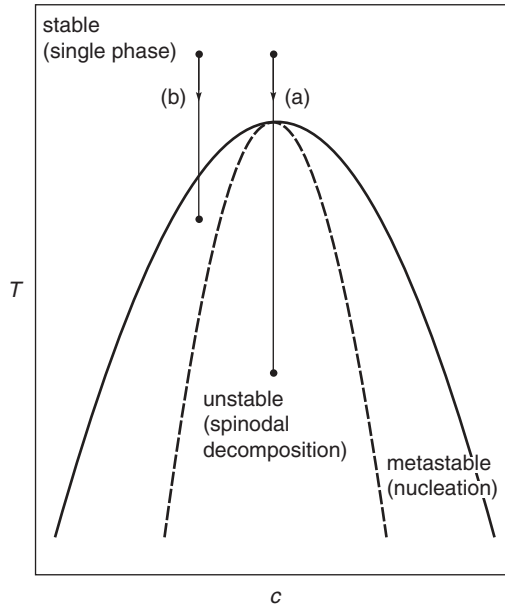


Fig. 2.1. Binary mixture phase diagram in the concentration–temperature plane showing critical (path a) and off-critical (path b) quenches into the two-phase region from the one-phase region. Path a starts at T_i and ends at T_f .

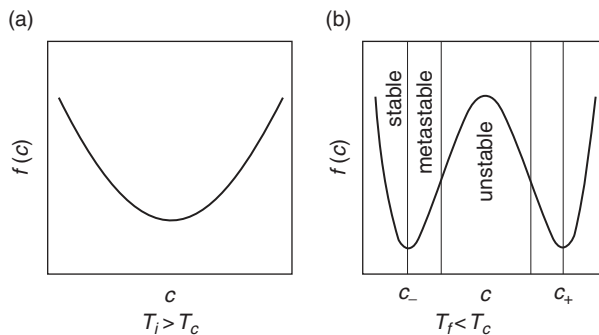


Fig. 2.2. Mean field free energy as a function of concentration for temperatures in the (a) one-phase and (b) two-phase regimes.

line may be generalized to any order parameter. A quench to a state within the spinodal region may lead to a labyrinthine pattern if it is associated with decay from an initial unstable state corresponding to the maximum in the free energy barrier. The evolution to a labyrinthine pattern is called spinodal decomposition. In contrast, an off-critical quench, such as the one shown as path b in Fig. 2.1, corresponds to evolution from an initial metastable state and involves a nucleation mechanism.

Both the morphology and phase separation dynamics depend crucially on the nature of the order parameter field. The order parameter may be conserved as in binary alloys or fluids, or nonconserved as in chemically reacting systems and antiphase domain growth in crystals. Dynamical models for the order parameter field that embody these conditions may be constructed and used to simulate phase separation dynamics. The system may require more than a single order parameter field for its description, and these order parameter fields may have different characters and symmetries. In such more general cases it may not be possible to define a free energy functional, and new phenomena may exist.

2.1 Mean field theory

2.1.1 Binary mixtures: alloys, fluids, and polymer blends

The specification of the thermodynamic state of a binary mixture requires three independent thermodynamic variables, say, the number density ρ , the concentration of the A species c and the temperature T . Only the (c, T) pair is relevant for the phase segregation process: thus, we consider a mixture of N_a molecules of type A and N_b molecules of type B with a fixed total number of molecules $N_o = N_a + N_b$ and fixed volume V . We define $c = N_a/N_o$, which implies $(1 - c) = N_b/N_o$. The differential Helmholtz free energy for a binary mixture may be expressed as

$$\begin{aligned} dF &= -SdT + \mu_a dN_a + \mu_b dN_b, \\ &= -SdT + N_o \mu dc, \end{aligned} \quad (2.1)$$

where the fixed N_o constraint is used in the second equality and $\mu = (\mu_a - \mu_b)$. It follows that the differential of the free energy per molecule $f = F/N_o$ is

$$df = -sdT + \mu dc, \quad (2.2)$$

where $s = S/N_o$. From this equation one can deduce that

$$\mu = \left(\frac{\partial f}{\partial c} \right)_T. \quad (2.3)$$

The chemical potential μ is thermodynamically conjugate to c , and the product of such a conjugate pair has dimensions of energy. The equation of state specifies the functional dependence among the three variables $\mu = \mu(c, T)$ and defines a surface in the three-dimensional (c, T, μ) space. A projection of this surface in the (c, T) plane was sketched in Fig. 2.1. The binary mixture critical point (c_c, T_c) is at the apex of the coexistence curve and is also referred to as the consolute point.

2.1 Mean field theory

9

There are two other projections of the equation-of-state surface. The (μ, T) projection consists of two regions: a homogeneous A -rich-phase region and a homogeneous B -rich-phase region. The two are separated by a monotonically increasing coexistence line of first-order phase transitions, which ends at the critical/consolute point, (μ_c, T_c) . The three coordinates of the critical point are obtained by simultaneously solving the following three equations:

$$\left(\frac{\partial \mu}{\partial c}\right)_{T=T_c} = 0, \quad \left(\frac{\partial^2 \mu}{\partial c^2}\right)_{T=T_c} = 0, \quad \mu_c = \mu(c_c, T_c). \quad (2.4)$$

The projection on the (μ, c) plane reveals what the (μ, T) projection hides, and it is useful to consider the behavior of isotherms in this plane. To gain an understanding of the qualitative structure of the chemical potential $\mu(c, T)$, consider the free energy functions sketched in Fig. 2.2. Differentiation of these functions with respect to c will result in two isotherms, one for the one-phase region and the other for the two-phase region. The isotherm for the one-phase region is monotonic and starts with a negative value of μ for small c . It becomes zero at the free energy minimum and increases monotonically to positive values of μ beyond the minimum. In contrast, the two-phase isotherm has a so-called van der Waals loop, since the free energy has three extrema at which μ vanishes.

To examine these features quantitatively, consider an analytic free energy function obtained from a mean field theory of a binary mixture (Bragg and Williams, 1934; Bethe, 1935; Huang, 1987),

$$\frac{f(c, T)}{k_B T} = c \ln(c) + (1 - c) \ln(1 - c) + \chi c(1 - c). \quad (2.5)$$

The first two terms in this function arise from the increase in the translational entropy due to mixing. In the last term, χ is a parameter describing the enthalpic interaction between the two species. For small molecules it is

$$\chi = \frac{z}{k_B T} \left[\epsilon_{AB} - \frac{1}{2}(\epsilon_{AA} + \epsilon_{BB}) \right], \quad (2.6)$$

where z is the effective coordination number and ϵ_{ij} is the interaction energy between monomers of species i and j . It is straightforward to obtain the corresponding chemical potential

$$\begin{aligned} \frac{\mu(c, T)}{k_B T} &= \ln(c) - \ln(1 - c) - \chi(2c - 1), \\ &= 2 \tanh^{-1}(2c - 1) - \chi(2c - 1). \end{aligned} \quad (2.7)$$

By equating each of the first two derivatives of μ with respect to c to zero, one finds $c_c = 1/2$, $\chi_c = 2$ and $\mu_c = 0$. Since $\chi = \chi(T)$, one can obtain T_c from χ_c . If χ is large and positive, phase segregation is favorable. The $\tanh^{-1}(x)$ function increases monotonically from $-\infty$ to $+\infty$ as x goes from -1 to $+1$. For small χ (high T), the linear term in Eq. (2.7) does not change the monotonic nature of μ ; however, for $\chi > \chi_c$, one obtains a van der Waals loop.

In the region around the critical point, it is appropriate to expand the free energy in powers of $c^* = (c - c_c)$. At the critical point $f_c/(k_B T_c) = \frac{1}{2} + \ln(\frac{1}{2})$, and the Taylor series expansion leads to the result

$$\frac{f(c^*, T)}{k_B T} - \frac{f_c}{k_B T_c} = \frac{a_2}{2} c^{*2} + \frac{a_4}{4} c^{*4} + \dots \quad (2.8)$$

where $a_2 = 2(\chi_c - \chi)$, which is proportional to $T - T_c$ for $\chi \sim T^{-1}$, and $a_4 = \frac{16}{3}$. This expansion is an example of what is generically called a Landau expansion of the free energy around the critical point.

An A - B polymer blend is a binary mixture of long-chain polymer molecules, and Flory-Huggins (FH) theory is a mean field theory for such a polymer mixture. In FH theory, polymer chains are placed on a lattice in such a way that each monomer unit occupies a lattice site, and connected polymer chains are placed so that they are locally self-avoiding. For an incompressible blend, all lattice sites are occupied by either A or B monomers. Let N_A (N_B) be the number of monomers (degree of polymerization) in an A (B) polymer chain. If c is the concentration of A in the polymer blend, the free energy of mixing per site for an incompressible blend is

$$\frac{f(c, T)}{k_B T} = \frac{c}{N_A} \ln(c) + \frac{(1-c)}{N_B} \ln(1-c) + \chi c(1-c), \quad (2.9)$$

where the Flory interaction parameter χ depends on c and T in a more complicated way than that for small molecule mixtures. It is often empirically fitted to a form $\chi = a + (b/T)$. The equation of state now takes the form

$$\frac{\mu(c, T)}{k_B T} = (N_A^{-1} - N_B^{-1}) + N_A^{-1} \ln(c) - N_B^{-1} \ln(1-c) + \chi(1-2c). \quad (2.10)$$

For a symmetric polymer blend ($N_A = N_B = N$) the critical point coordinates are $\mu_c = 0$, $c_c = 1/2$, $\chi_c = 2/N$. More generally, for non-symmetric polymer blends, $c_c = N_B^{1/2}/(N_A^{1/2} + N_B^{1/2})$, $\chi_c = (N_A^{1/2} + N_B^{1/2})^2/(2N_A N_B)$. The Landau expansion for a symmetric blend has the same form as that for the small molecules with $a_2 = 2(\chi_c - \chi)$ and $a_4 = 16/3N$. Many blends have an upper critical point where the blend is miscible for $\chi < \chi_c$ ($T > T_c$) and immiscible for $\chi > \chi_c$ ($T < T_c$) at the critical concentration c_c . Two limiting cases of a phase-separated blend are